POLITECNICO DI TORINO
Repository ISTITUZIONALE

Comprehensive Visualization of Data Generated by Fiber Bragg Grating Sensors

Terms of use:

Publisher copyright

(Article begins on next page)

27 April 2024

RESEARCH ARTICLE

Comprehensive Visualization of Data Generated by Fiber Bragg Grating Sensors

ANTONIO COSTANTINO MARCEDDU[1], (Graduate Student Member, IEEE),
ALESSANDRO AIMASSO[2], (Graduate Student Member, IEEE), **SERGIO SCHIAVELLO**[1],
BARTOLOMEO MONTRUCCHIO[1], (Senior Member, IEEE),
PAOLO MAGGIORE[2], (Member, IEEE),
AND MATTEO DAVIDE LORENZO DALLA VEDOVA[2], (Member, IEEE)

[1]Department of Control and Computer Engineering, Politecnico di Torino, 10129 Turin, Italy
[2]Department of Mechanical and Aerospace Engineering, Politecnico di Torino, 10129 Turin, Italy

Corresponding author: Antonio Costantino Marceddu (antonio.marceddu@polito.it)

ABSTRACT Testing is essential to validate the effort put into building a new system. In engineering fields such as aerospace, marine, mechanical, and others, these tests are particularly important for evaluating the overall safety level of the system. A crucial role is therefore played by sensors: in particular, they are required to function correctly even if exposed to harsh environments. In this regard, fiber optic-based sensors can meet this requirement successfully. However, it is necessary to use tools that allow the data collected to be displayed in real or near real-time and in such a way that they can be easily interpreted by an operator. This paper introduces new software that simplifies the visualization of data from fiber Bragg grating sensors. Despite traditional configuration, it works in wireless modality. It allows to range between visualization modes such as graphs and tables, and multiple functions for merging data from different measurements and more, useful for carrying out tests with greater awareness of what is happening at a given moment. The software has been successfully tested and verified in several case studies, ranging from laboratory analysis to telemetry testing of an Unmanned Aerial Vehicle (UAV) flight.

INDEX TERMS Aircraft, computer graphics, data visualization, databases, Fiber Bragg grating sensors, graphical user interfaces, middleware, optical fiber sensors, wireless communication.

I. INTRODUCTION

During the development of an engineering system it is always required to perform careful testing and validation of the system itself [1]. In particular, it is essential to monitor the performance of system components [2] while subjected to operating and environmental conditions similar to those under which it should normally operate [3], [4]. Although common to all engineering sectors, the testing phase is especially important for systems designed to operate in hostile or extreme environmental conditions [5], above all to preserve the electrical and electronic components [6]. This is a common requirement for aerospace systems [7], which are also requested to guarantee high efficiency in

The associate editor coordinating the review of this manuscript and approving it for publication was Mauro Fadda.

terms of lightness, minimum dimensions, or electromagnetic compatibility depending on the specific application [8].

In this regard, it becomes crucial to place sensors able to meet these requirements [9]. Due to the physical properties of the optical fiber [10], sensors based on it are considered innovative for aerospace because they meet all the aforementioned requirements [11] and can provide significant benefits [12]. In addition to being extremely lightweight and inexpensive, the cables are relatively small and, contextually, a large number of sensors can be integrated into the same communication line. Furthermore, and perhaps most importantly, the fiber is immune to electromagnetic interference and can function properly at cryogenic as well as extremely high temperatures [13]. Finally, it is chemically inert and electrically passive, ensuring that there are no sparks or potential fire starters [14].

This brief overview explains why optical fiber technology is important for the development of sensors capable of operating in the harsh environmental conditions typical of the aerospace sector. At *Politecnico di Torino* several research activities have been conducted about the features and advantages of using optical sensors for aerospace applications with a particular focus on *Fiber Bragg Grating* (FBG) sensors [15], [16] [17]. Studying their behavior requires feature-rich software, but most of them are often unable to provide all the relevant data for the ongoing analysis.

Therefore, this paper wants to propose a novel software to perform this type of operation called *PhotoNext FBG Data Analyzer*. Among its functions, there is the possibility of setting the typology of each FBG sensor detected, the presence of multiple data view modes, the possibility of calculating the Fast Fourier Transform (FFT), and more. Unlike other similar software on the market, *PhotoNext FBG Data Analyzer* is released as an open-source solution, usable as it is or freely modifiable in order to adapt it to fulfill the desired task [18]. The paper is organized as follows. Section II presents the operation of fiber optics with an emphasis on FBG sensors. Section III describes the previous work done by the authors of this paper, which helps to better understand the positioning of this research in relation to previous ones. Section IV discusses the different features offered by *PhotoNext FBG Data Analyzer*. The Sections V and VI report some tests of the software functionalities carried out both in the laboratory and in the field. Finally, Section VII reports the conclusions concerning the work done and a brief mention of future developments.

II. STATE OF THE ART ANALYSIS

Optical fiber is a mixed polymeric and glass material that can internally conduct a light signal [19]. As shown in Figure 1, it typically presents a cylindrical section and it is made up of three concentric layers, from inside to outside, called *core*, *cladding*, and *coating*. Due to the extreme fragility of the inner layers, the outer *coating* only provides structural functions. It is composed of a polymeric material and it could vary depending on the application. The *core* and *cladding*, on the other hand, are the innermost glass layers that allow the fiber to correctly function [20]. If the light enters properly into the *core*, when it reaches the interface between the two layers it undergoes a total internal reflection, which confines it to the *core*, so propagating the optical information along the fiber [21]. In the applications described in this work, only FBG sensors are used. These are generally obtained by laser photo-incision of a short trait (< 1 cm) of optical fiber [19]. This process generates a periodic re-modulation of the refractive index of the *core* [22], [23]: in this way, a structure called *Bragg grating* is created. The grating acts as a frequency-selective mirror: when the light beam passes through it, all frequencies of the electromagnetic spectrum can overcome the sensor, while a specific frequency is reflected in the opposite direction. This reflected frequency,
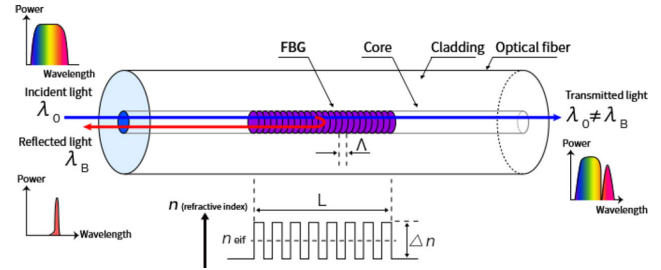

FIGURE 1. FBG structure and working principle. Image taken from [24].

called *Bragg frequency*, represents the output of the sensor and it is quantified in terms of wavelength:

$$\lambda_b = 2n_{eff} * \Lambda \tag{1}$$

where λ_b is the Bragg wavelength, n_{eff} is the modified refractive index of the core and Λ is the *grating pitch*. The pitch is the physical distance between two consecutive refractive index re-modulation of the *core*. The proportionality between the optical output of the FBG and its geometry allows for the correlation of a wavelength variation with a variation of a physical quantity acting on the sensor. In general, these two parameters are the temperature and the mechanical strain. So, it is possible to write the general equation governing the FBG response as follows:

$$\frac{\Delta\lambda}{\lambda_B} = K_T \Delta T + K_\varepsilon \Delta_\varepsilon \tag{2}$$

where:

- $\Delta\lambda = \lambda_i - \lambda_0$ is the wavelength variation of the i-measure from a reference value λ_0.
- $\Delta T = T_i - T_0$ is the thermal variation of the i-measure from a reference value T_0.
- $\Delta\varepsilon = \varepsilon_i - \varepsilon_0$ is the strain variation of the i-measure from a reference value ε_0.
- λ_B is the Bragg frequency.
- K_T is the temperature proportionality coefficient.
- K_ε is the strain proportionality coefficient.

More in detail, when sensors are put in condition to be sensitive only to temperature or strain, they can measure these parameters according to the following equations:

$$T_i = \frac{(\lambda_i - \lambda_0)}{(\lambda_B * K_T)} \tag{3}$$

$$\varepsilon_i = \frac{(\lambda_i - \lambda_0)}{(\lambda_B * K_\varepsilon)} \tag{4}$$

Optical fiber, as specified, has significant advantages for monitoring different physical parameters in system engineering activities. In particular, the great lightness, the versatility, and the minimal cable size allow the optical fiber to be employed even in radically different applications and/or systems. In addition, given its purely optical nature, it does not present electromagnetic compatibility problems: it can therefore be installed in proximity of electrical and electronic components and/or cables without risking

suffering or generating interference problems. The glassy composition of the optical fiber, moreover, ensures that it can also operate at extremely high temperatures (several hundred degrees) and without the possibility of generating sparks and thus possible fires. The combination of these characteristics, therefore, together with the high sensitivity to parameters such as temperature, strain, vibrations, etc., make optical sensors particularly suitable for ensuring high performance even when used in a hostile environment: a requirement, the latter, typical of the aerospace sector and, more generally, of the most complex and frontier engineering projects [25].

However, a crucial aspect is the user's capability of decoupling thermal and mechanical effects acting on the sensors. If this cannot be achieved, the use of FBGs may not be possible both in aerospace and other applications [26], [27]. In the case of a sensor exposed both to temperature and strain (as in the general case of (2)), it is possible to filter the contribution of a specific parameter (i.e. temperature) by subtracting the quantity $\Delta\lambda/\lambda_B$ from an FBG exposed only to temperature and then calculating the strain using (4).

In the experimental tests conducted by the authors of this paper, an instrument called *interrogator* was used: in particular, the *SmartScan* model produced by *Smart Fibres* was used. It generates a laser beam that is sent through the connected optical fibers. As previously mentioned, when the laser beam reaches the FBG gratings they reflect a specific frequency. This reflected frequency returns to the interrogator and it is quantified in terms of wavelength.

In the traditional configuration where the SmartSoft software provided by the manufacturer is employed [28], depicted in Figure 2, there are some significant limitations that make it challenging to use the technology for testing complex systems. In particular, the following issues are noted:

- Data tracking and related real-time graphs are possible for only few seconds and depending on the set acquisition frequency.
- Real-time combination of data from different sensors, such as thermal compensation for strain sensors, is not possible.
- The graphical representation is not very intuitive and lacks a time reference on the x-axis.
- It is necessary to connect the interrogator to the Personal Computer (PC) via Ethernet cable for data transmission and storage, which is incompatible with operations on flying test benches.

The software described in this paper attempts to overcome these issues. Before discussing it in detail, the work previously presented by the authors of this paper will be mentioned. Having complete knowledge of the entire infrastructure in which the software operates will indeed make it clearer to understand its operation.
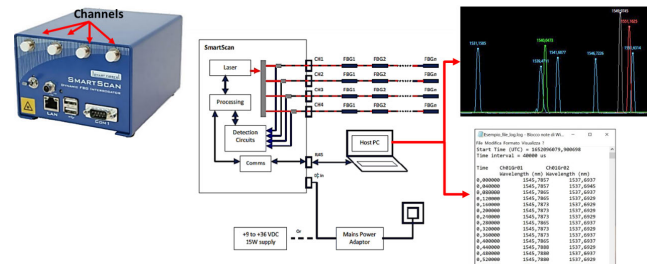

FIGURE 2. Scheme of traditional optical data acquisition system.

III. FLYING TEST BENCH

Last year, the authors of this paper published what has been dubbed as a *flying test bench* for FBG sensors [29], [30], [31]. It can be divided into two main parts:

- *Physical system*, composed of an instrumented aircraft model and the telemetry and acquisition system.
- *Software applications*, which read, transmit, store, and intuitively display the data coming from the FBG sensors.

A. PHYSICAL SYSTEM

The *physical system* is mainly composed of an instrumented model aircraft called *Anubi*. In one of its half-wings, there are 12 FBG sensors divided into three different lines. Their value is measured by a *SmartScan* interrogator, realized by *Smart Fibres*, and it is subsequently forwarded via Ethernet to a System-On-Chip (SOC), usually represented by a *Raspberry Pi™ 3 Model B+*. Both the interrogator and the SOC are powered by external batteries. All the previously described elements, except the SOC, are housed in the internal cavity of *Anubis* to improve the airflow around the model aircraft itself.

B. SOFTWARE APPLICATIONS

The *software applications* pipeline will be orderly discussed in the next lines.

The *PhotoNext Middleware* is a C/C++ Linux application capable of receiving from the interrogator peak data coming from the FBG sensors and retransmitting them to the *Cloud Database*. As for the flying test bench, this application normally operates on an Internet-enabled *Raspberry Pi™ 3 Model B+* via a *4G Internet Link Key*.

The *Cloud Database* is an instance of *MongoDB®* in charge of receiving the sensor data coming from the *PhotoNext Middleware* and sending them to all the *3D Viewer* active applications. This is possible through the Change Stream function offered by *MongoDB®*.

The *PhotoNext 3D Viewer* is a C# application built with Unity able to intuitively show the sensor data coming from the *Cloud Database* to the users of the flying test bench located on the ground. This is done using both a heat-mapped 3D representation and a graphical representation, both showing the difference of the value currently measured by the sensor compared to its resting value, called $\Delta\lambda$.
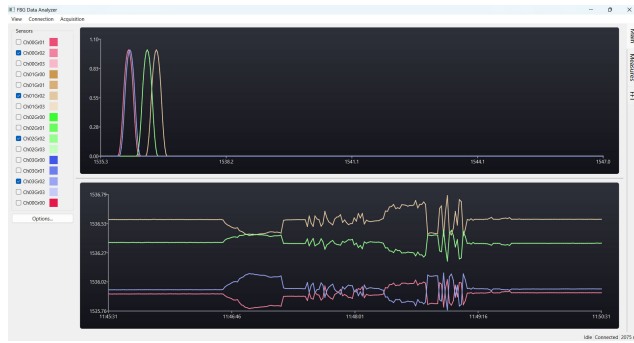
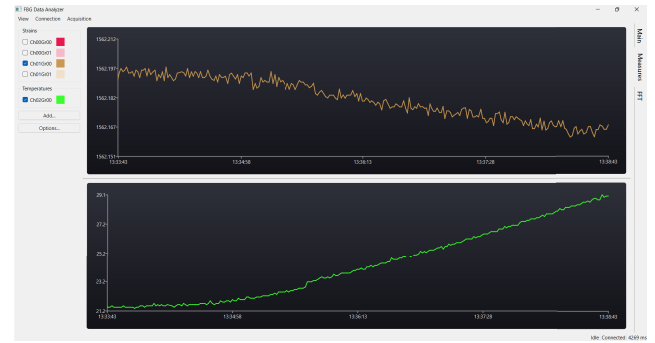**FIGURE 3.** A screenshot of the Main view of the *PhotoNext FBG Data Analyzer*.

FIGURE 4. A screenshot of the *Measures* view of the *PhotoNext FBG Data Analyzer*.

C. PREFACE TO THE NEXT SECTION

This summary of the functioning of the entire system is useful to better understand the level on which the discussion will focus, which is that of visualization. The software that will be introduced there, called *PhotoNext FBG Data Analyzer*, is an alternative version of the *PhotoNext 3D Viewer* that loses the ability to visualize data using a heat-mapped 3D representation in favor of multiple additions, which will be described in the next section [32].

IV. PHOTONEXT FBG DATA ANALYZER

The *PhotoNext FBG Data Analyzer* is a software developed in C++ through the use of the Qt framework [33]. Its purpose is similar to that of the *PhotoNext 3D Viewer*: it allows the operator to read FBG sensor data and other related information in a human-readable manner. Depending on the type of connection, this reading operation can be performed in real-time or near real-time. In fact, it is possible to read the sensor data through the connection to the *Cloud Database*, which is based on the Change Stream technology of *MongoDB®*, or through a Transmission Control Protocol (TCP) connection with a *PhotoNext Middleware* application located in the same local network. *PhotoNext FBG Data Analyzer* was developed with the aim of creating a richer and lighter version of the *PhotoNext 3D Viewer*. However, this required sacrificing the ability to show sensor data through the use of a heat-mapped 3D visualization.

A. VIEWS

The *PhotoNext FBG Data Analyzer* software is divided into three different views, which are accessible through the tab located on the right of the window. There is also an additional view that can be opened and positioned at will.

1) MAIN VIEW

The *Main view* can be used to see the instantaneous peak wavelength measured by the FBG sensors along with their trend over time. As it can be seen from Figure 3, it can be divided into three sections:

- On the left of the window it is possible to see the list of all the sensors detected by the system and the active

ones. It is automatically populated when the connection with the data source is established. The checkboxes allow choosing whether or not to display the data from a certain sensor, while the colored boxes allow choosing the color in which they will be shown.
- On the top-center of the window it is possible to see the graph reporting the instantaneous peak wavelength measured by the FBG sensors. If the mouse is moved over one of the peaks, a label showing the corresponding value will be shown. There is also a scroll mode, which allows viewing older data, not visible in the current window. It can be activated by hovering over the graph with the mouse pointer and using the touchpad scroll gesture or mouse scroll wheel. It is possible to exit this mode and go back to the live one by scrolling back to the last data received or by simply double-clicking on the graph.
- On the bottom-center of the window it is possible to see the graph reporting the peak wavelength measured by the FBG sensors over time.

The options button opens a new window that allows the user to enable or disable the automatic recalculation of the range, the grid, and more. The two graphs can be resized as desired by moving the separator between them, even seeing only one. They will also automatically resize according to the size of the software window.

2) MEASURES VIEW

The *Measures view* can be used to see the temperature or strain measured by the FBG sensors over time. As it can be seen from Figure 4, at first sight it is quite similar to the *Main view*, but it has big differences in uses:

- On the left of the window it is possible to add FBG sensors and select their type (a measure of temperature or strain). Depending on this, it will be possible to configure the respective proportionality coefficient and the starting reference value (k_T and T_0 for temperature and k_ε and ε_0 for strain) according to (3) and (4). In the latter case, it is also possible to fill the optional *field T*, which can be useful for indicating the sensor to be used as a temperature reference to compensate for the strain
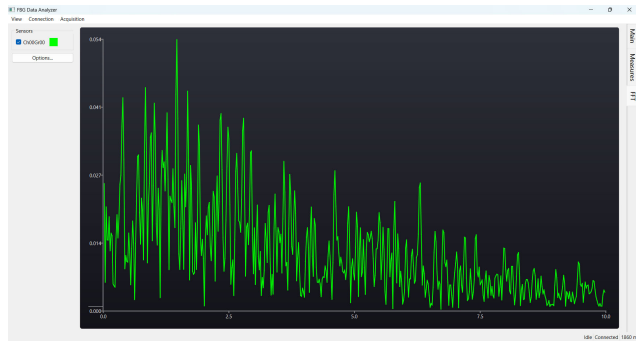
FIGURE 5. A screenshot of the FFT view of the *PhotoNext FBG Data Analyzer*.

FIGURE 6. A screenshot of the table view of the *PhotoNext FBG Data Analyzer*.

read. This is because both measurement variations play a role in the Bragg wavelength change.

- The graphs, which have the same features as the graphs in the *Main view*, display the strain and temperature measurements separately.

3) FFT VIEW

The *FFT view* allows the user to see the spectrum of the desired sensors. As it can be seen from Figure 5, the interface is not too different from the other views, but as already said before the graph shows the spectrum, which is calculated using the Fast Fourier Transformation (FFT). After an adequate testing phase, it was decided not to recalculate the FFT at the arrival of each new sample, but at the arrival of n new samples. This complies with the initial conditions for creating the software, which required optimization of the performance of the software. The options button opens a new window that allows the user to modify the sampling of the signal, the number *n* of samples on which to calculate the FFT, and more.

B. MENU BAR

The *Menu Bar* of the application, located on the top of the window, allows to view data in a tabular fashion, establish a connection via *TCP* on the local network or *Cloud Database* and perform local logging.

1) TABLE

As it can be seen From Figure 6, the *Table* button opens an additional view which was meant to have a precise, instant visualization of the value of each detected sensor. Unlike the previous views, it has been designed to be opened in a separate window that can be positioned anywhere on the screen, eventually also in a second monitor.

2) CONNECTION

The *Connection* section allows choosing and configuring the type of connection to be used for retrieving the data read through the *PhotoNext Middleware*. The available options have been stated before and are based on *TCP* on the local network or *Cloud Database*. Regardless of the connection
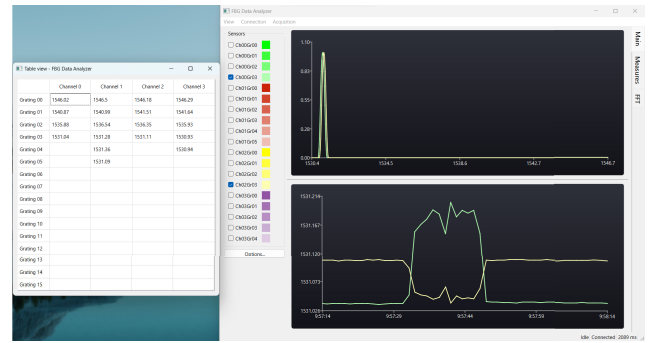
mode chosen, the connection status will be displayed in the bottom bar of the program. It can be one of the following: Disconnected, Connecting, or Connected. The delay with which data is received, always shown in the bottom bar of the software, will be constantly updated once the connection has been established, provided that data is actually being received.

3) ACQUISITION

The *Acquisition* section allows starting, stopping, and configuring the logging of the sensor data onto the local disk. In particular, it is possible to configure the sampling rate, the duration of the acquisition, and the subset of sensors to be logged. After having set these options it is possible to start and stop the acquisition by clicking on the homonymous buttons.

C. CONFIGURATION

All important information set by the user is automatically saved in the *settings.json* file, which is created when the software is executed for the first time. The user can also edit the software settings with a text editor and can create backup copies to create predefined templates that can be used in repeated measurement campaigns.

D. RELEASE

As anticipated in Section I, *PhotoNext FBG Data Analyzer* is distributed as an open-source solution that can be used as it is or freely modified to achieve the wanted task [18]. The development of the software was also made possible by using software capable of emulating the SmartScan interrogator, simply called *Emulator* [30].

V. LABORATORY TESTS

Some laboratory tests with the real interrogator and instrumentations were planned to validate the work made. They were conducted in an underground laboratory of the Politecnico di Torino by recurring to the following devices:

- A Windows 11 *laptop* connected to the Internet via a Wi-Fi hotspot and equipped with an AMD Ryzen 7 5700U CPU and 32GB of RAM was used to run the *PhotoNext FBG Data Analyzer*.

- a *Raspberry Pi™ 3 Model B+*, connected to the Internet via the same Wi-Fi hotspot of the laptop, was used to run the *Middleware*.
- The *SmartScan* by *Smart Fibres* was used as interrogator.
- The instrumented tail of the Anubi model aircraft was used to carry out tests relating to strain only.
- The *Beger KK-50 CHLT* was used as climatic chamber for temperature measurements.
- A *carbon fiber sample* and an *uncoated optical fiber sample* were used for performing temperature and strain measurements simultaneously.

A. STRAIN MEASUREMENT

This first test involved a strain measurement using the carbon fiber instrumented tail of the Anubi model aircraft. Four optical fibers were glued to it, two on the upper surface and two on the lower surface, each equipped with four FBG sensors placed at different heights along the tail.

For the execution of the experiments, the tail was constrained on the test bench using screws, nuts, and washers, and reinforced with an internally designed 3D-printed structure in SolidWorks. This was done to ensure that any externally applied loads would effectively stress the structure without causing the tail to simply rotate around its constraint on the bench. In addition, the test was conducted in a thermally controlled and constant environment, so that the optical change read by the instrumentation described in (2) could be rewritten as:

$$\frac{\Delta\lambda}{\lambda_B} = K_\varepsilon \Delta\varepsilon \tag{5}$$

in which the entire optical variation is due to the mechanical load applied to the sensor.

The full setting used to perform the strain measurement test is shown in Figure 7. For the sake of visual clarity, only 4 of the 16 strain sensors in the tail were represented in this test using the *PhotoNext FBG Data Analyzer*. They were then initialized with a k_ε of 0.01 and a ε_0 of 0 using the *Measures* view of the software. They represent the parameters needed to convert the optical output of the sensors into a physical value. The test was conducted by applying a variable load at the end of the tail through a specific support made of plastic material using additive manufacturing. The load was applied orthogonally to the tailplane, alternately acting upward and downward, in order to stress all the sensors in both tension and compression, thus verifying the correct functioning of the software.

The test results are visible in Figure 8. It is evident how the torsional stress induces compression on some fibers and tension on others, characterized respectively by a reduction and an increase in the wavelength detected by the sensor. Furthermore, the great sensitivity of the optical sensor in detecting extremely rapid transients in stress and the ability of the developed software to detect and graph the data appropriately is easily observable. This last capability is
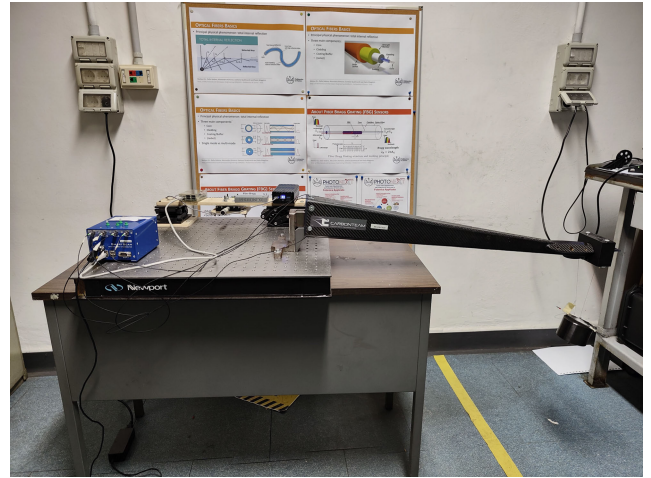

FIGURE 7. The setting used to conduct strain measurement test. It is possible to see the tail of Anubi, which is instrumented with optical sensors.

clearly visible in Figure 8, where the graphs generated in near real-time during the tests are compared with those produced during the post-processing phase after the conducted test activities.

B. TEMPERATURE MEASUREMENT

This second test involved a temperature measurement made using four different FBG sensors placed inside the climatic chamber. The aim was to check the legibility of multiple series on the *Measures* view chart of the *PhotoNext FBG Data Analyzer*. The setting used to perform the temperature measurement test is shown in Figure 9; since only thermal variations are applied to sensors, the optical output can be defined as follows:

$$\frac{\Delta\lambda}{\lambda_B} = K_T \Delta T \tag{6}$$

First, the FBG sensors were connected to channels 0 and 2 of the interrogator and placed inside the climatic chamber. The four temperature *sensors* were then initialized with a K_T of 0.01 and a T_0 of 25 using the *Measures* view of the *PhotoNext FBG Data Analyzer*. Subsequently, the following operations were carried out in an orderly manner:

1) The climatic chamber was preheated to $50°C$, giving both sensors time to adapt to this new situation.
2) Subsequently, the temperature inside the climatic chamber was lowered to $0°C$. As can also be seen in Figure 10, this led to a drop in the temperature measured by both sensors, which was correctly shown by the *PhotoNext FBG Data Analyzer* software.

The experiment was observed for about 20 minutes. From Figure 10 it is possible to see the gradual decrease in the measured temperatures. For three of the sensors it was rather similar, while the sensor connected to channel 1, represented in Figure 10 with an ochre color, measured a rather different value than the others. This difference in measurement, which
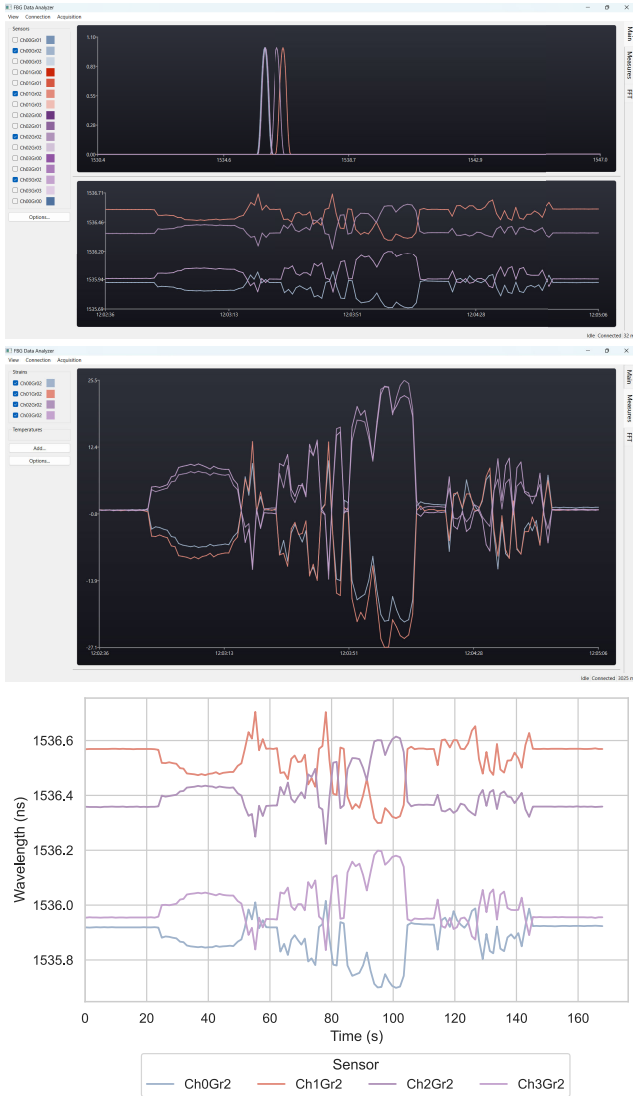
FIGURE 8. A comparison between the Main and Measures views of the *PhotoNext FBG Data Analyzer* during strain measurement test and post-processing analysis made on data saved on the *Cloud Database*.

also reaches differences of about $2°C$, it due to the use of a too-inaccurate degrees Celsius conversion constant.

C. STRAIN AND TEMPERATURE MEASUREMENT

This test was conducted with two different FBG sensors to verify the simultaneous display of two different types of measurements. Considering (2), when an FBG sensor is both mechanically stressed and subjected to a thermal transient, its output consists of the superposition of the two effects. To overcome this issue, it is necessary to complement this sensor with a second Bragg grating that is sensitive only to temperature. Assuming that the response of this last sensor is purely thermal, its output will be:

$$\frac{\Delta\lambda_c}{\lambda_B} = K_{TC}\Delta T \qquad (7)$$

FIGURE 9. The setting used to conduct temperature measurement test. It is possible to see the climating chamber containing the sensors network.

The response of the sensor subjected to both physical quantities, on the other hand, can be rewritten as (2), but calculating the environmental temperature from (7):

$$\frac{\Delta\lambda}{\lambda_B} = K_\varepsilon \Delta_\varepsilon + K_T \frac{\Delta\lambda_c}{K_{TC}} \qquad (8)$$

In this test, the aim is to verify the ability to measure strain and temperature using the compensatory technique just described through the produced software.

At first, the FBG sensors were connected to channels 1 and 2 of the interrogator. The *Measures* view of the *PhotoNext FBG Data Analyzer* was then configured as follows:

- The four strain *sensors* were initialized with a k_ε of 0.01 and a S_0 of 100.
- The temperature sensor was initialized with a k_T of 0.01 and a T_0 of 100.

Subsequently, the carbon fiber sample was used to measure the strain applied to it, while the uncoated optical fiber sample was inserted into the climatic chamber, which was configured to reach an internal temperature of $100°C$. From Figure 11 it can be seen that the latter, colored in purple, has measured an increasing temperature value, while the former was instead subjected to compressions and manual tractions of different entities. It can be clearly observed how the system is able to autonomously and reliably measure both the continuous, constant, and linear thermal variation and the mechanically applied load, increased in steps.
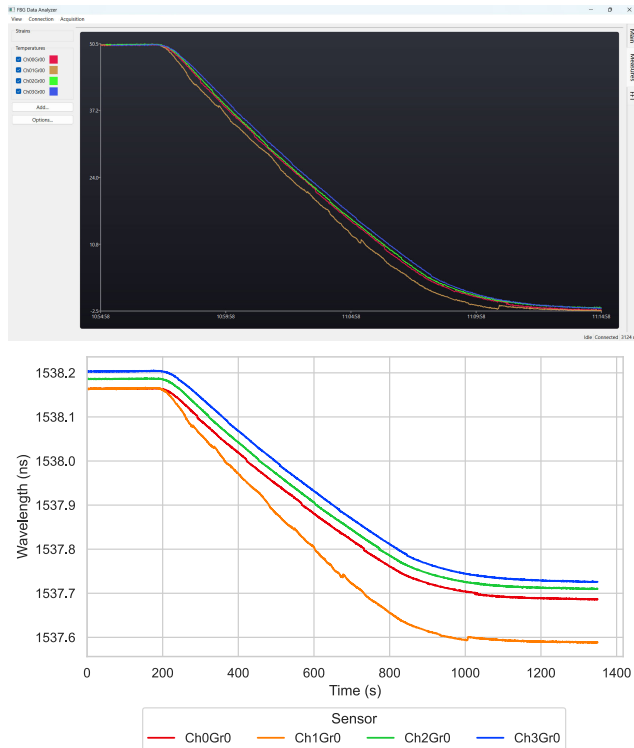
FIGURE 10. A comparison between the *Measures* view of the *PhotoNext FBG Data Analyzer* during temperature measurement test and post-processing analysis made on data saved on the *Cloud Database*. The program is able to convert wavelength to degrees Celsius for better visualization if the correct parameters are provided.

D. PERFORMANCE ANALYSIS

During the previously described tests, features such as latency, CPU (Central Processing Unit), and RAM (Random Access Memory) memory usage were monitored to analyze the performance of the *PhotoNext FBG Data Analyzer*.

1) LATENCY

The latency elapsed from the reception of the sensor data by the *PhotoNext Middleware* until its reception by the *PhotoNext FBG Data Analyzer* was calculated. This time was monitored with the aid of the relative indicator located in the software status bar. The tests reported in Sections V-A and V-B were conducted using the TCP connection mode. The minimum latency recorded was 13 *ms*, while the maximum was 62 *ms*. Instead, the test reported in the section V-C was conducted using the Cloud Database connection mode. In this case, the minimum latency recorded was 2658 *ms*, while the maximum was 4587 *ms*. As might be expected, the direct TCP connection offers the lowest latencies, but the Cloud Database connection offers acceptable latencies for most measurement campaigns. For the latter case, the saturation of the cell due to the high number of people in the university and the position of the laboratory have not helped to obtain the best results, however they can be drastically reduced by switching to a wired Internet connection.
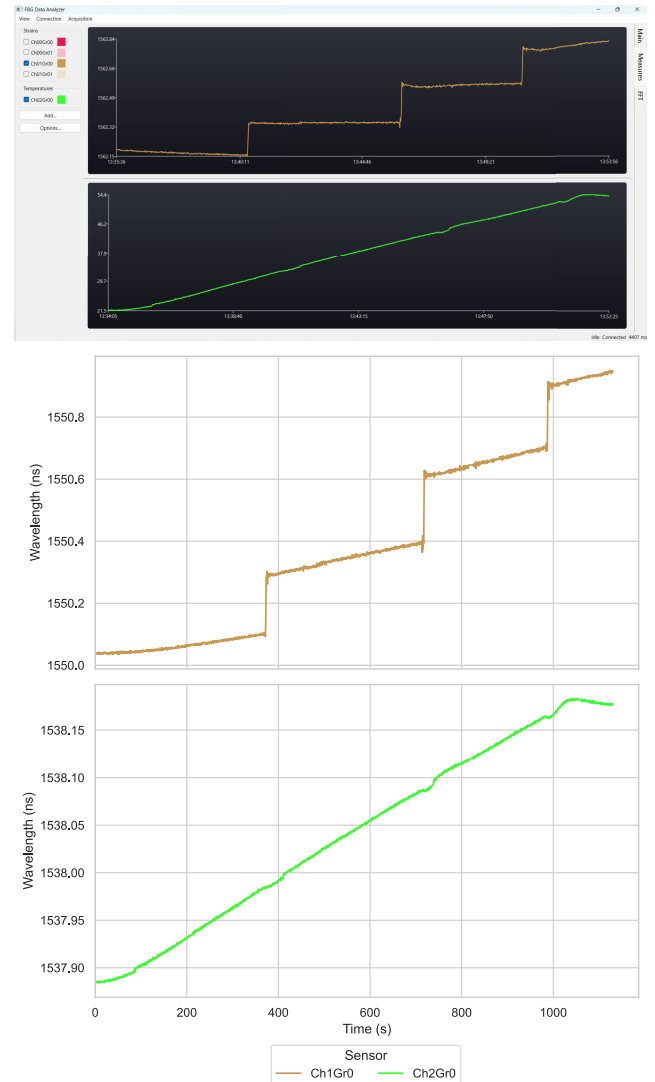

FIGURE 11. A comparison between the *Measures* view of the *PhotoNext FBG Data Analyzer* during simultaneous strain (in brown for the selected sensor) and temperature measurement (in green) test and post-processing analysis made on data saved on the *Cloud Database*.

2) CPU AND RAM USAGE

CPU and RAM usage of *PhotoNext FBG Data Analyzer* was monitored through the Process Explorer application, created by Mark Russinovich and other developers and distributed by Microsoft [34]. It allows seeing CPU, RAM, and I/O (Input/Output) usage statistics of the software currently running on a computer.

The software is quite lightweight, with an average CPU usage ranging from 1% to 3% and with few peaks of up to about 7%. They are due to the scaling of the graph: the minimum and maximum ranges are constantly monitored and possibly adapted to a range that allows the correct visualization of the new input data.

The same analysis can be performed regarding memory usage. After an initial period of growth, it stabilized at around 26 *MB*. This is due to the limit of points that are stored by the software for display purposes: when this value is reached, the

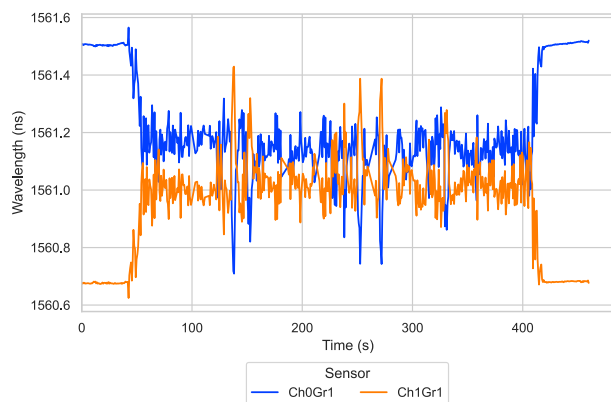**FIGURE 12. Flight test stand assembly procedures for the flight test.**

FIGURE 13. Comparison between *PhotoNext FBG Data Analyzer* near real-time data visualization during flight tests and post-processing analysis made on data saved on the *Cloud Database*.

internal buffer behaves as a FIFO (i.e. First In First Out), i.e. for each new element added to the buffer, the least recent.

VI. FLIGHT TESTS

The final verification of the reliability of the *PhotoNext FBG Data Analyzer* software was conducted through a flight test. The software was then connected to the aforementioned *physical system*, which can be remembered as being composed of the Anubi model aircraft and all the devices necessary to allow the in-flight data acquisition. Figure 12 shows a shot taken during the preparation of the flight test bench.

The FBG sensors used for this test were placed along the main spar of one of the two wings, both on the upper and the lower faces. In this way, due to aerodynamic loads, tensile and compressing loads can be observed symmetrically. Without

going too far into the physical details relative to the flight mechanics, it is useful to remark how each maneuver of the airplane generates a variation of the aerodynamic load acting on the wing. This load variation, consequently, leads to a different deflection of the wing over time and therefore to a varying deformation field. Having glued FBG sensors right along the airfoil, these deformations are then transferred to the optical sensors and thus measured, transferred, and displayed by the set of hardware and software that makes up the system.

In Figure 13 it is possible to observe the graphical output provided by the *PhotoNext FBG Data Analyzer*. The trend is successfully matched with graphs representing data saved in the database and realized after the conclusion of the test. As already noted for the previous cases, in this last test the software developed proved to be sufficiently robust to be used effectively in achieving the aims of the research group and in other similar applications. While only confirming what has already been demonstrated in the previous phases, verification through a flight test proved to be of paramount importance, as the level of complexity of this test is high enough to extensively test all the functionalities of the software.

VII. CONCLUSION

This paper presented an innovative visualization tool, called *PhotoNext FBG Data Analyzer*, created to simplify the study and analysis of FBG sensor data. It was built to be a lighter yet richer alternative to the previously used viewer, called *PhotoNext 3D Viewer*. The strengths of the developed software lie in the extreme intuitiveness of the graphical interface, coupled with the ability to perform data visualization and storage functions not available in the basic software provided by the hardware manufacturer. In particular, the developed product is designed to quantitatively graph and display, in real-time or near real-time depending on the connection, both the optical data provided by FBG sensors and the same parameter converted into a temperature or mechanical deformation value. Moreover, more complex functions are also available, such as FFT analysis or sensor data fusion processes for thermal compensation of deformation sensor data. Tabular schematization and trend data visualization complete the overview of the proposed functionalities.

All functions have been tested and verified, first in the laboratory through static and dynamic tests, and secondly through a flight test. The software has proven to be able to reproduce and improve the performance provided by the software currently provided with the instrumentation, allowing for wireless data telemetry and monitoring. This represents the most challenging result: it was not possible with the standard software and it is essential for testing innovative engineering systems in the aerospace sector.

Finally, future activities include further improving the software by adding support for monitoring various physical parameters (pressure, altitude, humidity, accelerations) measured with FBG sensors.

REFERENCES

[1] S. R. Hirshorn, L. D. Voss, and L. K. Bromley, "NASA systems engineering handbook," Nat. Aeronaut. Space Admin. (NASA), Washington, DC, USA, Tech. Rep. HQ-E-DAA-TN38707, 2017.

[2] R. Quigley, "More electric aircraft," in *Proc. 8th Annu. Appl. Power Electron. Conf. Expo.*, 1993, pp. 906–911.

[3] R. J. Sayer. *New Testing Methods can Benefit Mechanical Systems.* Accessed: Oct. 30, 2023. [Online]. Available: https://www.reliableplant.com/Read/28645/new-testing-methods

[4] D. Belmonte, M. D. L. D. Vedova, and P. Maggiore, "Prognostics of onboard electromechanical actuators: A new approach based on spectral analysis techniques," *Int. Rev. Aerosp. Eng.*, vol. 11, no. 3, pp. 96–103, Jun. 2018.

[5] N. Staff. *Microsystems for Harsh Environment Testing | NIST.* Accessed: Oct. 30, 2023. [Online]. Available: https://www.nist.gov/programs-projects/microsystems-harsh-environment-testing

[6] V. Peesapati, L. Fang, R. Giussani, and I. Cotton, "Comparison of standards requirements for clearances in aerospace," in *Proc. IEEE Electr. Insul. Conf. (EIC)*, Jun. 2013, pp. 434–438.

[7] D. Wright, Z. Stephenson, and M. Beeby. *Safety Through Quality Efficient Verification Through the DO-178C Life Cycle.* Accessed: Oct. 30, 2023. [Online]. Available: https://www.rapitasystems.com/files/MC-WP-011%20DO-178C%20Verification_2.pdf

[8] F. Ciampa, P. Mahmoodi, F. Pinto, and M. Meo, "Recent advances in active infrared thermography for non-destructive testing of aerospace components," *Sensors*, vol. 18, no. 2, p. 609, Feb. 2018. [Online]. Available: https://www.mdpi.com/1424-8220/18/2/609

[9] F. Eggers, J. H. S. Almeida Jr., T. V. Lisbôa, and S. C. Amico, "Creep and residual properties of filament-wound composite rings under radial compression in harsh environments," *Polymers*, vol. 13, no. 1, p. 33, Dec. 2020. [Online]. Available: https://www.mdpi.com/2073-4360/13/1/33

[10] M. J. Matthewson, "Optical fiber mechanical testing techniques," in *Proc. Fiber Opt. Rel. Test., Crit. Rev.*, vol. 10272, D. K. Paul, Ed., 1993, Art. no. 1027205, doi: 10.1117/12.181373.

[11] S. Mihailov, D. Grobnic, C. Hnatovsky, R. Walker, P. Lu, D. Coulas, and H. Ding, "Extreme environment sensing using femtosecond laser-inscribed fiber Bragg gratings," *Sensors*, vol. 17, no. 12, p. 2909, Dec. 2017. [Online]. Available: https://www.mdpi.com/1424-8220/17/12/2909

[12] A. Behbahani, M. Pakmehr, and W. A. Stange, "Optical communications and sensing for avionics," in *Springer Handbook of Optical Networks.* Cham, Switzerland: Springer, 2020, pp. 1125–1150.

[13] R. Rodríguez-Garrido, A. Carballar, J. Vera, J. González-Aguilar, A. Altamirano, A. Loureiro, and D. Pereira, "High-temperature monitoring in central receiver concentrating solar power plants with femtosecond-laser inscribed FBG," *Sensors*, vol. 21, no. 11, p. 3762, May 2021.

[14] A. Wosniok, D. Skoczowsky, M. Schukar, S. Pötzsch, S. Pötschke, and S. Krüger, "Fiber optic sensors for high-temperature measurements on composite tanks in fire," *J. Civil Struct. Health Monitor.*, vol. 9, no. 3, pp. 361–368, Jul. 2019.

[15] A. Aimasso, M. D. L. D. Vedova, P. Maggiore, and G. Quattrocchi, "Study of FBG-based optical sensors for thermal measurements in aerospace applications," *J. Phys., Conf. Ser.*, vol. 2293, no. 1, Jun. 2022, Art. no. 012006.

[16] A. Aimasso, M. D. L. D. Vedova, and P. Maggiore, "Innovative sensor networks for massive distributed thermal measurements in space applications under different environmental testing conditions," in *Proc. IEEE 9th Int. Workshop Metrol. Aerosp. (MetroAeroSpace)*, Jun. 2022, pp. 503–508.

[17] M. D. L. Dalla Vedova, P. C. Berri, and A. Aimasso, "Environmental sensitivity of fiber Bragg grating sensors for aerospace prognostics," in *Proc. 31st Eur. Saf. Rel. Conf. (ESREL)*, 2021, pp. 1561–1567.

[18] Politecnico di Torino. *PhotoNext FBG Data Analyzer.* Accessed: Oct. 30, 2023. [Online]. Available: https://github.com/CARDIGANSPoliTo/PhotoNext_FBG_Data_Analyzer

[19] S. J. Mihailov, "Fiber Bragg grating sensors for harsh environments," *Sensors*, vol. 12, no. 2, pp. 1898–1918, Feb. 2012. [Online]. Available: https://www.mdpi.com/1424-8220/12/2/1898

[20] H. Alemohammad, "Opto-mechanical modeling of fiber Bragg grating sensors," in *Opto-Mechanical Fiber Optic Sensors Research, Technology, and Applications in Mechanical Sensing.* Oxford, U.K.: Butterworth-Heinemann, Jan. 2018, pp. 1–26.

[21] S. Kasap, *Optoelectronics and Photonics: Principles and Practices.* Upper Saddle River, NJ, USA: Prentice-Hall, 2001.

[22] K. Tankala, "Reliability of low-index polymer coated double-clad fibers used in fiber lasers and amplifiers," *Opt. Eng.*, vol. 50, no. 11, Nov. 2011, Art. no. 111607, doi: 10.1117/1.3615653.

[23] G. P. Agrawal and S. Radic, "Phase-shifted fiber Bragg gratings and their application for wavelength demultiplexing," *IEEE Photon. Technol. Lett.*, vol. 6, no. 8, pp. 995–997, Aug. 1994.

[24] T. Staff. *FBG | Optical Products (Photo Devices) | Sensors and Medical Products | Products and Services | Tatsuta Electric Wire and Cable Co., Ltd.* Accessed: Oct. 30, 2023. [Online]. Available: https://www.tatsuta.com/product/sensor_medical/optical/fbg/

[25] A. Aimasso, C. G. Ferro, M. Bertone, M. D. L. D. Vedova, and P. Maggiore, "Fiber Bragg grating sensor networks enhance the in situ real-time monitoring capabilities of MLI thermal blankets for space applications," *Micromachines*, vol. 14, no. 5, p. 926, Apr. 2023. [Online]. Available: https://www.mdpi.com/2072-666X/14/5/926

[26] F. Attivissimo, F. Adamo, L. De Palma, D. Lotano, and A. Di Nisio, "First experimental tests on the prototype of a capacitive oil level sensor for aeronautical applications," *Acta IMEKO*, vol. 12, no. 1, pp. 1–6, Feb. 2023. [Online]. Available: https://acta.imeko.org/index.php/acta-imeko/article/view/1474

[27] S. de Gioia, F. Adamo, F. Attivissimo, D. Lotano, and A. Di Nisio, "A design strategy for performance improvement of capacitive sensors for in-flight oil-level monitoring aboard helicopters," *Measurement*, vol. 208, Feb. 2023, Art. no. 112476. [Online]. Available: https://www.sciencedirect.com/science/article/pii/S0263224123000404

[28] Smart Fibres. *Smartsoft Application Software.* Accessed: Oct. 30, 2023. [Online]. Available: https://www.smartfibres.com/files/pdf/SmartSoft-for-SmartScan.pdf

[29] A. C. Marceddu, G. Quattrocchi, A. Aimasso, E. Giusto, L. Baldo, M. G. Vakili, M. D. L. D. Vedova, B. Montrucchio, and P. Maggiore, "Air-to-ground transmission and near real-time visualization of FBG sensor data via cloud database," *IEEE Sensors J.*, vol. 23, no. 2, pp. 1613–1622, Jan. 2023.

[30] A. C. Marceddu, A. Aimasso, A. Scaldaferri, P. Maggiore, B. Montrucchio, and M. D. L. D. Vedova, "Creation of a support software for the development of a system for sending and visualizing FBG sensor data for aerospace application," in *Proc. IEEE 10th Int. Workshop Metrol. Aerosp. (MetroAeroSpace)*, Jun. 2023, pp. 487–491.

[31] A. C. Marceddu and B. Montrucchio, "Storage and visualization on-the-ground and in near real-time of the data measured by the optical sensors connected to a flying test bench," in *Proc. Mater. Res.*, vol. 33, 2023, pp. 277–280.

[32] S. Schiavello, "Innovative visualization of data generated by photonic sensors," M.S. thesis, Sergio Schiavello, Politecnico di Torino, 2022.

[33] The Qt Company. *Qt.* Accessed: Oct. 30, 2023. [Online]. Available: https://www.qt.io/

[34] M. Russinovich. *Process Explorer.* Accessed: Oct. 30, 2023. [Online]. Available: https://learn.microsoft.com/en-us/sysinternals/downloads/process-explorer

ANTONIO COSTANTINO MARCEDDU (Graduate Student Member, IEEE) received the B.Sc. and M.Sc. degrees in computer engineering from Politecnico di Torino, in 2015 and 2019, respectively, where he is currently pursuing the Ph.D. degree under the supervision of Prof. Bartolomeo Montrucchio. Before the Ph.D. degree, he was a Research Assistant. His research interests include machine learning, computer vision, data visualization, and quantum computing.

ALESSANDRO AIMASSO (Graduate Student Member, IEEE) received the M.Sc. degree in aerospace engineering from Politecnico di Torino, in 2020, with a specialization in the space sector, where he is currently pursuing the Ph.D. degree with the Department of Mechanics and Aerospace Engineering (DIMEAS). Before the Ph.D. degree, he was a Researcher. His current research interests include optic sensors integrations in both aeronautical and space systems.

SERGIO SCHIAVELLO received the B.Sc. and M.Sc. degrees in computer engineering from Politecnico di Torino, in 2020 and 2022, respectively. He has been working in the telecommunications industry for the railway sector for the past six years, currently as a Software Developer, following three years holding the position of the IT Manager.

BARTOLOMEO MONTRUCCHIO (Senior Member, IEEE) received the M.Sc. degree in electronic engineering and the Ph.D. degree in computer engineering from Politecnico di Torino, Turin, Italy, in 1998 and 2002, respectively. He is currently a Full Professor in computer engineering with the Department of Control and Computer Engineering, Politecnico di Torino. His current research interests include image analysis and synthesis techniques, scientific visualization, sensor networks, RFIDs, and quantum computing.

PAOLO MAGGIORE (Member, IEEE) received the M.Sc. degree in aerospace engineering from Politecnico di Torino, in 1988. In 1992, he joined the Department of Mechanical and Aerospace Engineering, Politecnico di Torino, where he is currently a Professor in aerospace general systems engineering. His research interests include hydrogen-fuel-cell-powered airplanes and UAV, the health monitoring of electromechanical flight controls to the multidisciplinary design optimization of aerospace system design.

MATTEO DAVIDE LORENZO DALLA VEDOVA (Member, IEEE) received the M.Sc. and Ph.D. degrees in aerospace engineering from Politecnico di Torino, in 2003 and 2007, respectively. He is currently an Assistant Professor with the Department of Mechanics and Aerospace Engineering. His research activity is focused on aeronautical systems engineering, including the design, analysis, and numerical simulation of on board systems, secondary flight control systems and related monitoring strategies, and the development of prognostic algorithms for aerospace servomechanism.

• • •